

# A Study of the 23 October 2022 Southern England Damaging MCS

Kenneth Pryor, David Smart, David Flack, Matthew Clark

## Abstract

During the afternoon of 23 October 2022, a mesoscale convective system (MCS) developed and intensified over the English Channel and tracked north-northeastward into southern England, producing widespread damaging winds and at least three moderate to strong tornadoes in Hampshire. In general, atmospheric temperature and moisture profiles from radiosonde observations and NOAA satellites indicated a high potential for severe thunderstorm, straight line wind, and tornado occurrence over southern England. Radar and satellite observed coincidentally high rain rates and very low storm-top temperatures as well as prominent trends in MCS organization and intensity that suggested damaging outflow wind.

## Introduction

Cool-season convective storms over northwestern Europe and Great Britain continue to be a forecasting challenge as well as a public safety hazard, especially during periods of unseasonably warm temperatures and associated enhanced instability. Among the most common cool-season storms are the mesoscale convective system (MCS), defined as a deep convective system that is considerably larger than an individual thunderstorm and that is often marked by an extensive middle to upper tropospheric stratiform-anvil cloud of several hundred kilometers in horizontal dimension (Cotton and Anthes 1992). Severe windstorms (i.e., widespread convective wind gusts  $> 25.7 \text{ ms}^{-1}$  (50 kt)) resulting from MCSs cause significant disruption to society, including widespread power grid damage, tree and structural damage, and transportation disruptions that affect metropolitan areas along their track. A rear-inflow jet into an MCS (Smull and Houze Jr., 1987; Weisman, 1992), which channels unsaturated mid-tropospheric air into the leading convective storm line, increases the likelihood of severe convective winds resulting from downbursts. Downbursts are strong downdrafts that induce an outburst of damaging winds at or near the ground (Fujita, 1985; Wakimoto, 1985). The establishment of an elevated, ascending front-to-rear flow originating from deep, moist convection, overlying a strong and deep outflow-induced cold pool has been found to generate and sustain a robust rear inflow jet (Weisman, 1992) and perpetuate downburst generation through the mature stage of the MCS. The imposition of a strong wind shear field in the cool-season MCS environment can foster tornadogenesis as intense convective outflow focuses boundary layer convergence and vorticity on the system's leading edge.

During the afternoon of 23 October 2022, an MCS, with a morphological evolution more typical of the warm season over continental Europe (Gatzen 2004; Mathias et al. 2017), developed and intensified over the English Channel and tracked north-northeastward into southern England. The combination of atypically large potential instability and vertical wind shear established over central and southern England during the afternoon and the structural characteristics of the convective elements of the system promoted the development of four tornadoes and damaging downburst winds in five counties and greater London over a three-hour period (Horton 2023a, Horton 2023b). The favorable dynamic factors revealed in this study warrant further investigation

into the potential role of elevated convection and the development of a rear-inflow jet during the most intense phase of the system (Weisman 1992; White et al. 2016). Comparison of low-Earth orbit (LEO) satellite microwave imagery to Doppler radar reflectivity patterns and cross-sections of numerical weather prediction (NWP) model-derived thermodynamic parameters (i.e., CAPE ratio from the Met Office Unified Model (UM)) should further strengthen the evidence for MCS structure and the presence of a rear-inflow jet. Figure 1, a Met Office Global and Regional Ensemble Prediction System (MOGREPS)-UK (2.2 km resolution) model simulation of the MCS during its track between Hampshire and London highlights some of the favorable dynamic factors that promoted strong outflow wind generation (Pryor 2022a; Pryor 2022b): 1) precipitation loading, 2) downshear wake entrainment, and 3) rear-flank circulation and induced rear-inflow jet. More interestingly, surface analyses (not shown) revealed that the MCS developed and propagated within a warm seclusion and dry intrusion zone of a Shapiro-Keyser cyclone that possibly supported the potentially unstable environment as evident by the precipitation spatial patterns shown in Figure 1b.

This research effort demonstrates how ground-based and satellite-based observational data for convective storms can be combined for monitoring and forecasting applications while highlighting the scientific value added by synergistic analysis of satellite and ground-based sensor datasets. Among the most important tropospheric analysis and diagnostic tools is the NOAA-Unique Combined Atmospheric Processing System (NUCAPS, Nalli et al. 2020, Kalluri et al. 2022), an enterprise algorithm that retrieves atmospheric profiles of temperature and moisture and derived environmental stability parameters. NUCAPS, frequently applied and evaluated for both a daytime and nocturnal severe convective windstorm cases, is also the primary algorithm for the operational hyperspectral thermal infrared and microwave sounders onboard the United States NOAA and European Organisation for the Exploitation of Meteorological Satellites (EUMETSAT) operational low earth orbit satellites. For this study, NUCAPS sounding profiles, retrieved over Cornwall, West Sussex and Leicestershire, respectively, at midday (1222 UTC) were compared with co-located 1200 UTC radiosonde observation (RAOB) soundings. The NUCAPS soundings provided a lead time of three hours before the onset of the MCS over southern England.

Figure 2 illustrates the intensive data analysis and comparison process employed to infer and extract the most important physical processes that sustained the MCS and fostered intense outflow winds. The most important steps in the evaluation process entail pattern recognition, parameter evaluation, and feature identification applying coincident sounding retrieval and satellite, radar and NWP model 2-D plan-view images to build a three-dimensional conceptual model. Due to the optimal timing of satellite overpasses and attendant retrievals with respect to the most intense phase of the MCS, the United States Defense Meteorological Satellite Program (DMSP) F-16 and F-18 satellite Special Sensor Microwave Imager Sounder (SSMIS) datasets were employed to extract the most important patterns related to severe convection and downburst occurrence (See Pryor 2022b for a detailed description of the SSMIS instrument). SSMIS 91GHz window channel and the 150 GHz and 183 (+/- 7) GHz water vapor sounding channel datasets were obtained and applied for the purpose of storm microphysical analysis. For the SSMIS, dual-polarized 91 GHz brightness temperature datasets allow for calculating polarization-corrected temperature (“PCT”, Liu et al. 1995), while the difference between the horizontally-polarized 91 GHz and 150 GHz brightness temperature defines the scattering index (SI, Ferraro et al. 2000). In addition, National Weather Service Climate Prediction Center morphing technique (CMORPH) (<https://www.ncei.noaa.gov/products/climate-data-records/precipitation-cmorph>) precipitation

rate datasets were obtained and visualized to evaluate the overall morphology and intensity of the MCS. CMORPH (Joyce et al. 2004) uses motion vectors derived from half-hourly interval geostationary satellite IR imagery to propagate the relatively high-quality precipitation estimates derived from passive microwave data. In addition, the shape and intensity of the precipitation features are modified during the time between microwave sensor scans by performing a time-weighted linear interpolation to generate complete microwave-derived precipitation analyses, independent of the infrared temperature field. The most relevant usage and strength of the CMORPH global precipitation datasets is to supplement radar data in regions of non-existent or poor radar coverage (i.e., over oceans or sparsely developed continental regions) while CMORPH provides a regional perspective of precipitation systems without degradation due to attenuation, refraction, and other artifacts of the radar sampling process.

To compare directly with passive microwave sounding imagery, the UK currently has a network of 16 C-band, dual polarisation, Doppler radars. Short pulse data, with a maximum range of 115 km, are analysed from two radars in the storm impact area (Dean Hill and Chenies). The single site scans from these radars, with beam width 1 degree and range gates every 0.6 km, were capable of generating imagery with the resolution required to identify embedded mesoscale features of the MCS, including bow echoes, supercells, line-end and leading-line vortices.

## Dorset-Hampshire-Sussex, UK Bow Echo and Supercell<sup>1</sup>

The initial evolution of the MCS over southern England, denoted in Figure 3, entailed its track from the English Channel northward into Dorset and Hampshire between 1430 and 1500 UTC and development of a prominent bowing segment on its western (left) flank over the English Channel that persisted during its track through south-central England. The squall line bow echo (Klimowski et al. 2004) merged with a supercell storm over Bournemouth near 1445 UTC and then proceeded north-northeastward into Hampshire (not shown), producing a series of tornadoes and a severe downburst observed by a SYNOP station. The progression of the MCS through Hampshire between 1430 and 1530 UTC entailed a long-track (> 60 km) tornado from Barton on Sea to Hurstbourne Priors with a maximum of T2 to T3<sup>2</sup> strength (Horton 2023a). Simultaneously, an intense, but shorter track (~3.75 km) tornado of T2 to T3 strength (Horton 2023a) impacted the Marwell area from Horton Heath to Horsham Copse and was directly viewed by CCTV at Marwell Zoo (see BBC [news article](#) online). In addition, severe straight-line wind damage was reported to the adjacent west of the long-track tornado from Romsey to northwest of Stockbridge.

One significant downburst event during the MCS track through Hampshire was observed at 1515 UTC, at Middle Wallop Army Aviation Centre (88 km southwest of London) SYNOP station, in which a 54-kt ( $28 \text{ ms}^{-1}$ ) wind gust was recorded. Shortly after 1600 UTC, the SSMSIS PCT and 183 (+/- 7) GHz brightness temperature product images displayed the general bowing structure of the MCS and a prominent rear-inflow notch over Hampshire in Figure 4. Near this time, the bow-echo complex was moving through Wiltshire and Berkshire, succeeding the downburst wind event at Middle Wallop and the adjacent long-track tornado through Hampshire. Corresponding Doppler radar imagery, nearly 30 minutes prior at 1541 UTC, more clearly displayed the western bookend vortex and an area of localized rotation associated with the bow echo-supercell merger. The most compelling signatures apparent in radar were a distinct, localized

<sup>1</sup> "Dorset-Hampshire-Sussex" refers to the spatial extent of the MCS, not the direction of system motion.

<sup>2</sup> TORRO International tornado scale. See <https://www.torro.org.uk/research/tornadoes/tscale> for more details.

bow echo tracking immediately to the west of an embedded supercell in the larger scale northward-bowing configuration illustrated by the SSMIS brightness temperature imagery.

Storm-scale interaction and morphological evolution were effectively depicted in the CMORPH precipitation rate imagery in Figure 5 as the MCS was tracking through Dorset, Hampshire, and West Sussex between 1500 and 1600 UTC. The CMORPH precipitation imagery suggested the early phase of development of a trailing stratiform region that would become much more prominent during the London bow echo phase discussed in the next section. The remarkably low PCTs and 183 GHz channel BTs below 180 K signified the enhancement of mixed and ice-phase precipitation loading within the bow-echo complex (Klimowski et al. 2004) thereby further strengthening the system cold pool. Markowski (2002) reviewed the role of the convective downburst in the acceleration of the storm gust front, and the generation and enhancement of vertical vorticity at the interface between the downburst outflow and rotating updraft. The combined effect of these processes likely results in the intensification of a low-level mesocyclone and subsequent tornadogenesis. Doppler radar imagery most clearly indicated MCS-supercell mergers over Hampshire and the resulting bow echo enhancement following the process described by French and Parker (2012, “FP12”). The mergers over Hampshire closely resembled the “system-scale bowing evolution” based on radar reflectivity analysis as designated by FP12, and, in this case, was associated with the generation of severe downburst winds promoted by cold pool enhancement as well as squall line-induced tornadoes.

Figures 6, 7, and 8, a qualitative comparison of RAOB and NUCAPS sounding profiles over Cornwall and Sussex, revealed favorable conditions for intense storm downdraft generation and resultant strong outflow winds with close agreement between the boundary layer structure (“inverted-V”) as resolved by the NUCAPS soundings and the microburst windspeed potential index (MWPI, Pryor 2015) gust potential as calculated from NUCAPS. An additional step in the downburst wind gust potential calculation process was to add one-third (1/3) of the forward storm motion to the MWPI WGP (Miller 1972)<sup>3</sup>. In addition, the RAOB and NUCAPS soundings provided essential thermodynamic parameters for downburst and tornado potential assessment including the lower-to-middle tropospheric lapse rates, lifted condensation level (LCL), and wet bulb zero height. Following the technique of Pryor (2022a, 2022b), thermodynamic diagrams were also plotted with the virtual temperature correction to ultimately yield a stronger signal for severe convection and downburst generation. Since the resultant downdraft intensity in the boundary layer is dependent upon the difference between the downdraft parcel temperature and the environmental virtual temperature, the virtual temperature lapse rate is a more physically realistic expression to quantify downburst wind potential (Pryor, 2015; Srivastava, 1985).

The Camborne, Cornwall 1200 UTC RAOB shown in Figure 6 provided early indication for both strong outflow wind and tornado potential with a wet-bulb zero height near the 750 mb level and an LCL height of 582 m. Craven and Brooks (2004) noted in their study of sounding-derived parameters associated with moist convection that significant tornado environments featured 0–3 km above ground level (AGL) temperature lapse rates greater than  $6 \text{ C km}^{-1}$  and LCL heights below 1000 m. Miller (1972) states that a high probability of strong outflow winds exists when the wet-bulb zero height is located within the layer of 650 mb to 850 mb in a “type 1” air mass<sup>4</sup>. Very low LCLs enhance tornado potential by limiting sub-cloud evaporation and decreasing the potential for cold outflow that could interfere with the developing mesocyclone. The wet-bulb zero height serves as an indicator for the source level of convective downdrafts.

<sup>3</sup> Derived from Miller (1972) chapter 10, section A.

<sup>4</sup> Derived from Miller (1972) chapter 7.

Thus, the virtual temperature-corrected sounding profile at Camborne exhibited optimal conditions for tornadogenesis, combining the high potential for storm outflow balanced by a low LCL height. The corresponding NUCAPS sounding profile at Truro, Cornwall shown in Figure 7 indicated a lower tornado potential with an LCL height above 2000 m, despite illustrating favorable conditions for moderate downburst winds with a wet-bulb zero height near the 700 mb level and a deeper layer of potential instability. The NUCAPS profile retrieved over West Sussex at 1222 UTC and displayed in Figure 8 more closely matched the Camborne RAOB profile, while signifying a higher downburst wind gust potential ( $> 50$  kt ( $25.7 \text{ ms}^{-1}$ ), incorporating 1/3 of the storm motion) and a marginally low LCL height near 1100 m. These conditions were manifested in the proximate occurrence of the Hampshire long-track tornado generated by an embedded supercell and the downburst at Middle Wallop associated with a local-scale bow echo. The CAPE ratio (Flack et al. 2023) of zero calculated from the West Sussex NUCAPS sounding agreed well with Figure 9, the MUK model-derived CAPE ratio (defined as  $1 - (\text{SBCAPE}/\text{MUCAPE})$ ), indicating a high likelihood of surface-based convective storm development that would produce damaging downburst winds, especially near the bow echo apex. The 1600 UTC CAPE ratio product shown in Figure 9 signifies that generally low values of the ratio calculation ( $< 0.4$ ) favored hazardous surface-based convective storm development during the MCS track through the Greater London area and these conditions are discussed in more detail in the next section.

### **London and Southeastern England Bow Echo**

The MCS track from Wiltshire-Berkshire-Kent region to the Midlands between 1600 and 1800 UTC entailed a merger with a supercell over Greater London, representing the second instance of a noteworthy MCS-supercell merger of the severe storm event. As shown in Figures 10, 11, and 12, the MCS developed a prominent bowing segment west of London that persisted during the remainder of its track. Unlike the previous merger event over southern Hampshire, the MCS-supercell merger over London resulted in a cluster of large, intense convective storms that produced a succession of downbursts over Hertfordshire between 1640 and 1740 UTC. A broken line of discrete cells, some rotating, formed just ahead of the bowing segment of the MCS over parts of SE England. The MCS merged with these cells as it moved through the London area. In one case, the merger resulted in a small bowing line segment and associated localised region of strong outflow winds (evident in radial velocity data). The core of this feature moved NNE just to the west of the Phoenix Model Club (“PMC”), London Colney, Hertfordshire, where a gust of 56 kt ( $28.8 \text{ ms}^{-1}$ ) was observed at 1640 UTC. During this period, the stratiform precipitation region that commenced development between 1500 and 1600 UTC, increased in areal coverage and propagated in the wake of the embedded storm cluster. F-16 SSMIS 150 GHz retrievals were available for the pass over southeastern England, as shown in Figure 10, allowing for the calculation of the scattering index and the inference of the presence of anvil cirrus plumes immediately downshear of the leading convective storm line of the MCS. A similar signature was noted by Pryor (2022, 2022a) related to the track and evolution of the 29 June 2012 Derecho system that impacted the Washington, DC, US metropolitan area.

The general system-scale bowing of the squall line is still apparent in CMORPH imagery in Figure 11 with a marked increase in rainfall rate coincident with the track of the leading convective line over greater London. CMORPH imagery also shows an attendant increase in the precipitation rate gradient on the upshear flank of the trailing elevated convection region, suggesting an increase in rear inflow. Doppler radar velocity imagery in Figure 12 confirms the

increase in rear inflow toward the region of the MCS-supercell merger where a localized embedded bow echo developed over southern Hertfordshire. Shortly after the merger, the PMC downburst wind event was recorded by a WeatherFile sonic wind sensor.

Figures 13 and 14, the 1200 UTC Nottingham RAOB and the 1222 UTC Loughborough, Leicestershire NUCAPS sounding profiles, respectively, signified a higher favorability for intense storm downdraft generation and resultant strong outflow winds. In a similar manner to the West Sussex NUCAPS retrieval, the soundings at Leicestershire and Nottingham exhibit a higher downburst wind gust potential as indicated by wet bulb zero heights near the 750 mb level that correspond to a deep layer of potential instability. The calculated MWPI-derived gust potential of 58 kt ( $29.8 \text{ m s}^{-1}$ ) at Loughborough, Leicestershire (incorporating 1/3 of the storm motion) was very close to the magnitude of downburst winds recorded at London Colney. The calculated CAPE ratio values derived from the virtual temperature-corrected RAOB and NUCAPS sounding profiles increased to 0.29 – 0.37 corresponding closely to the UM-derived CAPE ratio values of 0.1-0.5 over the Midlands shown in Figure 15. The cessation of damaging wind reports during the continued track of the MCS north of Hertfordshire after 1800 UTC was possibly associated with a trend toward the favorability of elevated convection that was effectively indicated by the 1800 UTC CAPE ratio product image shown in Figure 15b.

## Discussion and Conclusions

The strategic application of polar-orbiting meteorological satellite and ground-based microwave (radar) datasets allowed for the comprehensive tracking of the MCS through most of its life-cycle. In addition to application of high-resolution, convection-allowing numerical prediction models, coordinated monitoring of the thermodynamic structure and associated stability of the lower troposphere with co-located satellite and ground-based sounding retrievals provided an effective operational demonstration.

In general, the early afternoon (1222 UTC) NOAA-20 NUCAPS sounding qualitatively indicated the strongest signal for severe thunderstorm and downburst occurrence over southern England: Close agreement between the boundary layer structure ("inverted-V") as resolved by the NUCAPS soundings and the MWPI gust potential as calculated from NUCAPS. A strong relationship is noted between high rain rates as indicated by UKMO radar, IMERG product imagery, and the very low MW brightness temperatures (BTs) apparent in both the consecutive F-18 and F-16 overpasses. Low BTs also correspond well with the high integrated graupel values, suggesting that intense downdrafts and resulting downbursts were forced by ice-phase precipitation loading and melting, as well as unsaturated air entrainment into the mixed-phase precipitation core.

Diagnostics to determine the environment that the convection formed in, from Flack et al. (2023), show that the event was initially surface-based. However, as time progressed and the convective cores stabilized the environment, the rear of parts of the MCS had elements of elevated instability influencing the convection. This elevated instability may help explain the increased precipitation rates within the stratiform region of the MCS and investigations are still ongoing. Future work will consist of further exploration of the role of squall line-supercell mergers in the enhancement and promotion of severe straight-line winds and tornadogenesis in close proximity. This phase of the study will likely entail higher resolution model simulations that are more sensitive to precipitation phase and concentration and boundary layer turbulence. In addition, the application of convolutional neural networks (CNNs) to the microwave brightness temperature

and CMORPH rainfall rate product imagery (via the use of edge detection filters) will be explored to evaluate the identification process of signatures favorable for severe outflow (downburst) winds and tornadogenesis within organized MCSs.

## Acknowledgements

The authors would like to thank Matthew Clark (TORRO/UK Met Office) for his thorough review of this manuscript and insightful comments in addition to his analysis and descriptive annotation of the Doppler radar imagery presented in Figures 4 and 12.

## References

- Bush, M., Boutle, I., Edwards, J., Finnenkoetter, A., Franklin, C., Hanley, K., Jayakumar, A., Lewis, H., Lock, A., Mittermaier, M., Mohandas, S., North, R., Porson, A., Roux, B., Webster, S., and Weeks, M. 2023: The second Met Office Unified Model–JULES Regional Atmosphere and Land configuration, RAL2, Geosci. Model Dev., 16, 1713–1734, <https://doi.org/10.5194/gmd-16-1713-2023>.
- Craven, J.P., H.E. Brooks, and J.A. Hart, 2004: Baseline climatology of sounding derived parameters associated with deep, moist convection. Natl. Weather Digest, 28, 13–24.
- Ferraro, R. R., F. Weng, N. C. Grody, and L. Zhao, 2000: Precipitation characteristics over land from the NOAA-15 AMSU sensor. Geophysical Research Letters, 27(17), pp.2669-2672.
- Flack, D.L.A., Lehnert, M., Lean, H.W., and Willington S. (2023) Characteristics of Diagnostics for Identifying Elevated Convection over the British Isles in a Convection-Allowing Model. Wea. Forecasting 38: 1079-1094, <https://doi.org/10.1175/WAF-D-22-0219.1>
- French, A. J., and M. D. Parker, 2012: Observations of Mergers between Squall Lines and Isolated Supercell Thunderstorms. Wea. Forecasting, 27, 255–278, <https://doi.org/10.1175/WAF-D-11-00058.1>
- Gatzen, C., 2004: A Derecho in Europe: Berlin, 10 July 2002. Wea. Forecasting, 19, 639–645, DOI: [https://doi.org/10.1175/1520-0434\(2004\)019<0639:ADIEBJ>2.0.CO;2](https://doi.org/10.1175/1520-0434(2004)019<0639:ADIEBJ>2.0.CO;2)
- Horton, S, 2023a: The Barton on Sea to Hurstbourne Priors Extended Tornado track 23 October 2022. TORRO site Investigation report: SI20221023\_BOS\_HP, [https://www.torro.org.uk/pdf/SI/SI20221023\\_BartononSea\\_to\\_HurstbournePriors.pdf](https://www.torro.org.uk/pdf/SI/SI20221023_BartononSea_to_HurstbournePriors.pdf)
- Horton, S, 2023b: The Marwell Tornado 23 October 2022. TORRO site Investigation report: SI20221026\_Marwell, [https://www.torro.org.uk/pdf/SI/SI20221023\\_Marwell.pdf](https://www.torro.org.uk/pdf/SI/SI20221023_Marwell.pdf)
- Joyce, R. J., J. E. Janowiak, P. A. Arkin, and P. Xie, 2004: CMORPH: A method that produces global precipitation estimates from passive microwave and infrared data at high spatial and temporal resolution.. J. Hydromet., 5, 487-503.

Kalluri, S., C. Barnet, M. Divakarla, R. Esmaili, N. Nalli, K. Pryor, T. Reale, N. Smith, C. Tan, T. Wang, J. Warner, M. Wilson, L. Zhou, and T. Zhu, 2022: Validation and Utility of Satellite Retrievals of Atmospheric Profiles in Detecting and Monitoring Significant Weather Events. *Bulletin of the American Meteorological Society*, 103, E570-E590, <https://doi.org/10.1175/BAMS-D-20-0126.1>

Klimowski, B. A., M. R. Hjelmfelt, and M. J. Bunkers, 2004: Radar Observations of the Early Evolution of Bow Echoes. *Wea. Forecasting*, 19, 727–734, [https://doi.org/10.1175/1520-0434\(2004\)019<0727:ROOTE>2.0.CO;2](https://doi.org/10.1175/1520-0434(2004)019<0727:ROOTE>2.0.CO;2).

Liu, G., J.A. Curry, and R.W. Sheu, 1995: Classification of clouds over the western equatorial Pacific Ocean using combined infrared and microwave satellite data. *Journal of Geophysical Research: Atmospheres*, 100(D7), 13811-13826.

Mathias, L., V. Ermert, F. D. Kelemen, P. Ludwig, and J. G. Pinto, 2017: Synoptic Analysis and Hindcast of an Intense Bow Echo in Western Europe: The 9 June 2014 Storm. *Wea. Forecasting*, 32, 1121–1141. DOI: 10.1175/WAF-D-16-0192.1

Miller, R.C., 1972: Notes on the analysis and severe-storm forecasting procedures of the Air Force Global Weather Central. *Air Weather Service Tech. Rept. 200 (Rev.)*, Air Weather Service, Scott Air Force Base, IL, 190 pp.

Nalli, N.R., C. Tan, J. Warner, M. Divakarla, A. Gambacorta, A.; M. Wilson, T. Zhu, T. Wang, Z. Wei, K. Pryor, S. Kalluri, L Zhou, C. Sweeney, B. C. Baier, K. McKain, D. Wunch, N. M. Deutscher, F. Hase, L. T. Iraci, R. Kivi, I. Morino, J. Notholt, H. Ohyama, D. F. Pollard, Y. Té, V. A. Velasco, T. Warneke, R. Sussmann, M. Rettinger, 2020: Validation of Carbon Trace Gas Profile Retrievals from the NOAA- Unique Combined Atmospheric Processing System for the Cross-Track Infrared Sounder. *Remote Sens.*, 12, 3245. <https://doi.org/10.3390/rs12193245>

Pryor, K. L., 2015: Progress and developments of downburst prediction applications of GOES. *Wea. Forecasting*, 30, 1182–1200, <https://doi.org/10.1175/WAF-D-14-00106.1>

Pryor, K. L., and B. Demoz, 2022: A Retrospective Satellite Analysis of the June 2012 North American Derecho. *Remote Sensing*, 14(14), 3479; <https://doi.org/10.3390/rs14143479>

Pryor, K. L., 2022a: Examination of the Physical Process of Severe Convective Windstorms [Doctoral dissertation]. University of Maryland, Baltimore County.

Pryor, K.L., 2022b: “Downburst monitoring and prediction studies”. *Field Measurements for Passive Environmental Remote Sensing*, Elsevier, Cambridge, MA, 2022, pp. 411–429.

Srivastava, R.C., 1985: A Simple Model of Evaporatively Driven Downdraft: Application to Microburst Downdraft. *J. Atmos. Sci.*, 42, 1004–1023.

Weisman, M. L., 1992: The role of convectively generated rear inflow jets in the evolution of long-lived mesoconvective systems. *J. Atmos. Sci.*, 49, 1826–1847.

White, B. A., A. M. Blyth, and J. H. Marsham, 2016: Simulations of an observed elevated mesoscale convective system over southern England during CSIP IOP 3. Q.J.R. Meteorol. Soc., 142, 1929–1947. <https://doi.org/10.1002/qj.2787>

## Figures

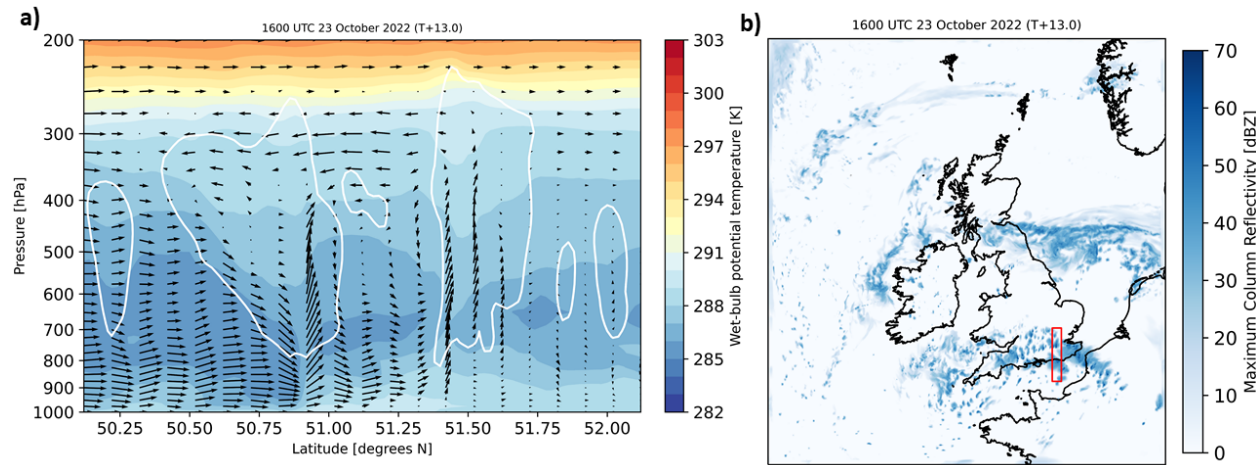


Figure 1. A deep convective storm with the potential to generate intense downdrafts and damaging downburst winds: a) cross-section and b) plan view of MUK (2.2 km) model-simulated radar reflectivity over Great Britain at 1600 UTC 23 October 2022. Plotted in the cross-section are wet-bulb potential temperature, system-relative wind vectors, and the total water content to indicate the cloud outline.

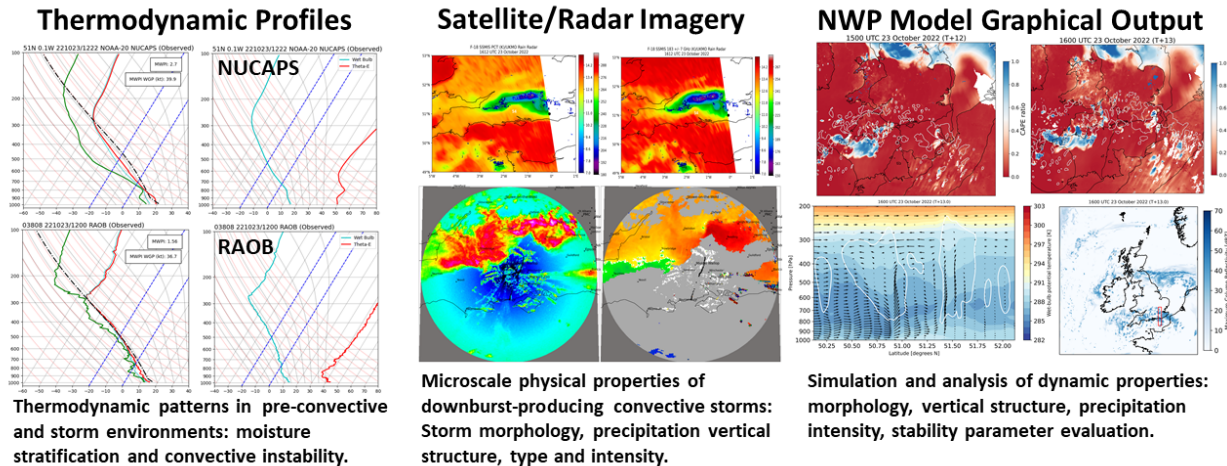


Figure 2. Graphical summary of data analysis and methodology for this study as applied to successive phases of the MCS. Examples of NUCAPS sounding (skew-T) profiles intercompared with RAOBs are shown in the left column; the middle column shows representative satellite microwave and radar images shortly after the tornadic phase of the MCS; the right column shows examples of derived NWP model product images and a vertical cross-section model of the MCS shortly before the greater London damaging phase of the MCS.

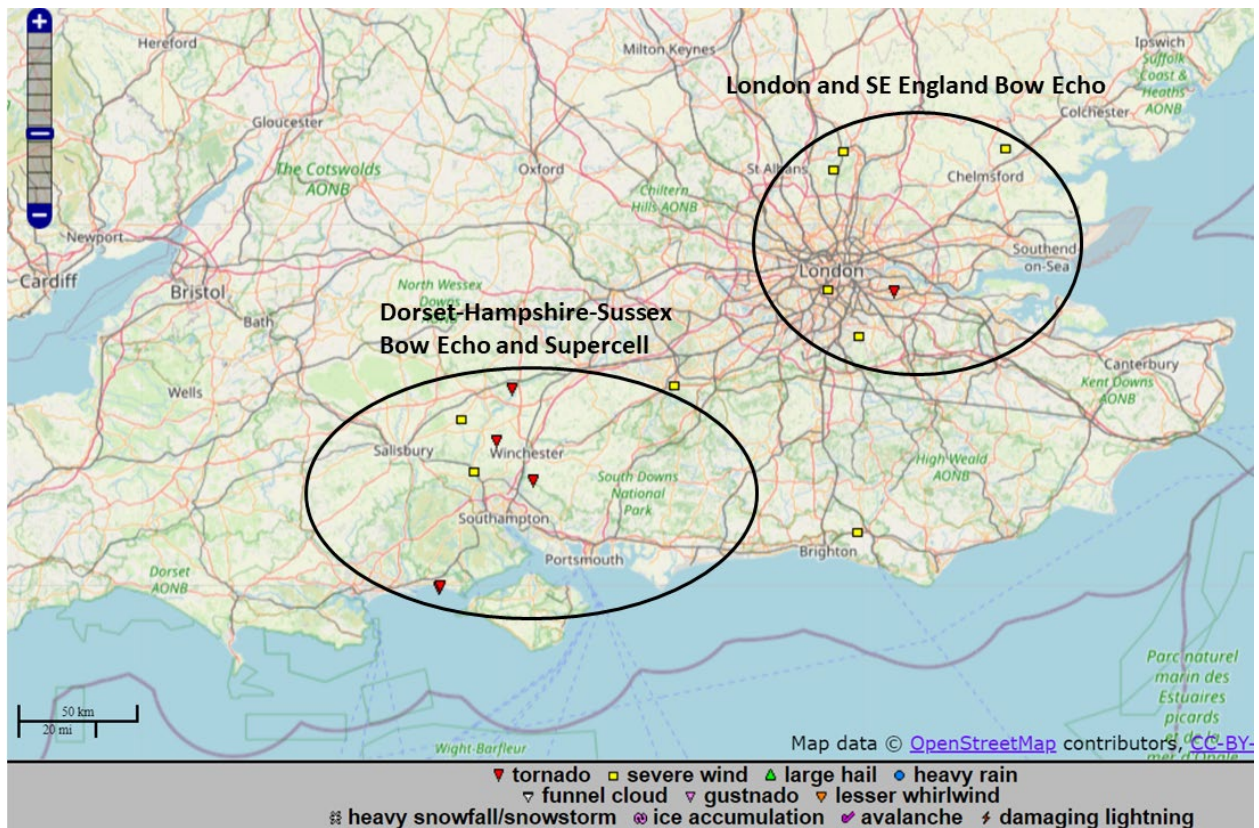


Figure 3. European Severe Weather Database (ESWD) storm reports over Great Britain on 23 October 2022 outlining two important phases of the MCS: 1) the Dorset-Hampshire-Sussex bow echo and long-track tornado from New Milton to Whitchurch, Hampshire and 2) the Greater London bow echo.

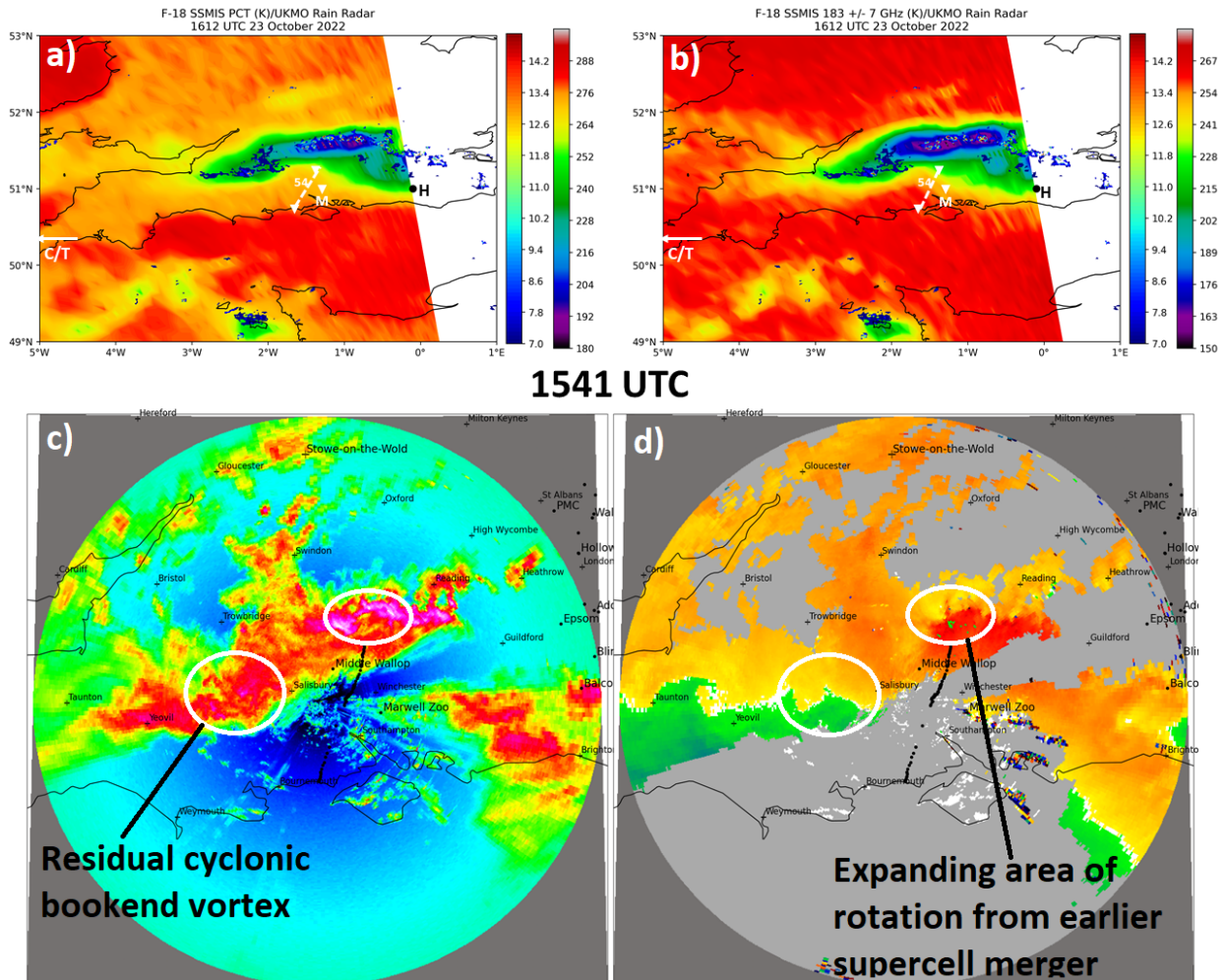


Figure 4. F-18 SSMIS a) polarization-corrected temperature (PCT, K) and b) 183 +/- 7 GHz brightness temperature with overlying UKMO radar rain rate at 1612 UTC 23 October 2022. Dean Hill, Wiltshire, UK Doppler radar c) reflectivity and d) velocity at 1541 UTC 23 October 2022. “C/T” denotes RAOB and NUCAPS sounding retrieval locations at Camborne and Truro, Cornwall, UK, respectively in a) and b). “H” marks the NUCAPS sounding retrieval location at Haywards Heath, West Sussex, UK. “M” marks the location of tornado impact at Marwell, Hampshire. The white dashed line represents the long-track tornado from Barton on Sea to Hurstbourne Priors, Hampshire while the adjacent “54” represents the 54-kt ( $28 \text{ ms}^{-1}$ ) downburst wind gust recorded at Middle Wallop Army Aviation Centre, Hampshire SYNOP station.

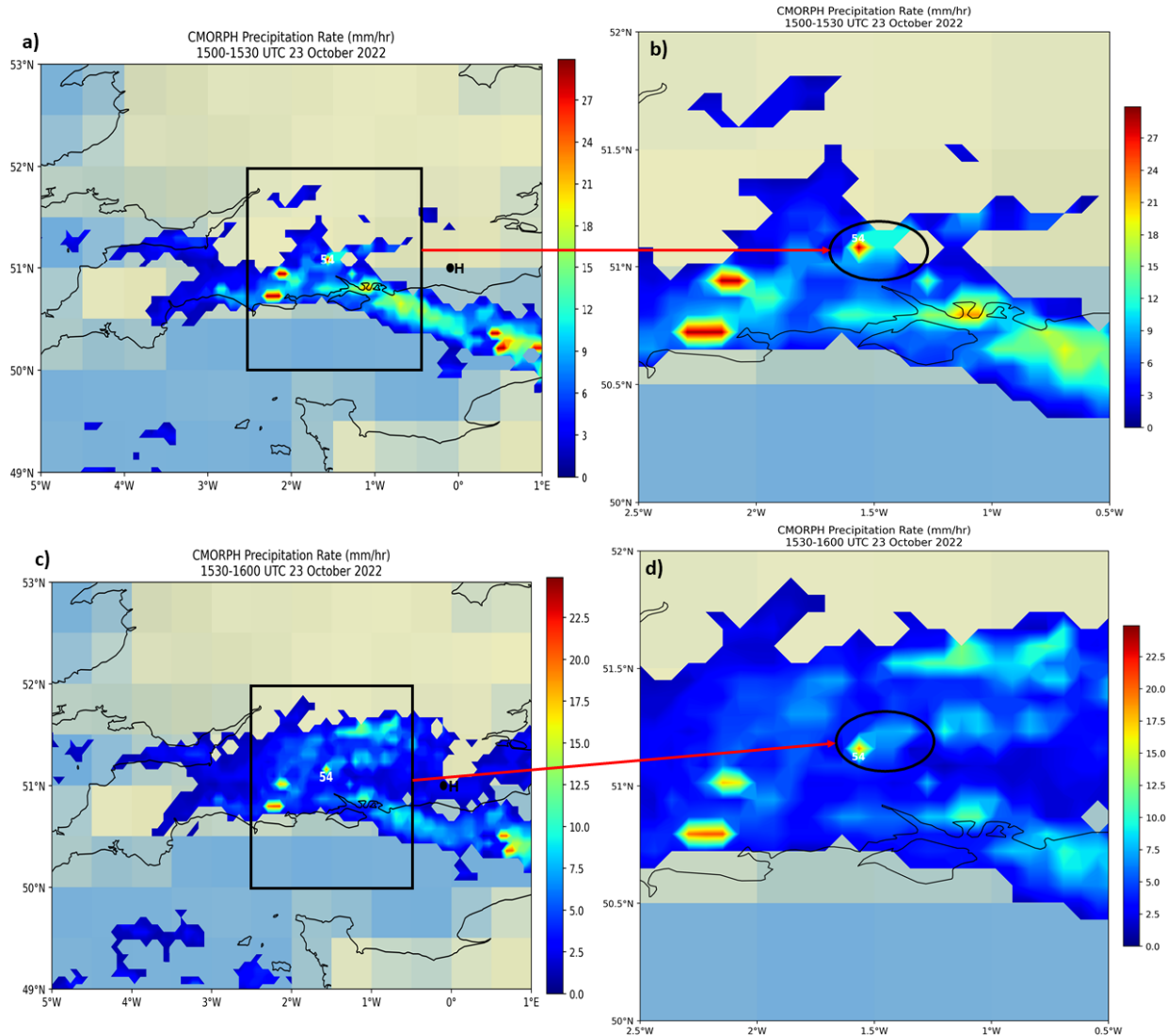


Figure 5. 23 October 2022 CMORPH precipitation rate (mm/hr) product imagery over southern Great Britain at a) 1500-1530 UTC and c) 1530–1600 UTC. South-central England sector precipitation rate product imagery at b) 1500-1530 UTC and d) 1530-1600 UTC. “54” represents the 54-kt ( $28 \text{ ms}^{-1}$ ) downburst wind gust recorded at Middle Wallop Army Aviation Centre, Hampshire SYNOP station. “H” marks the NUCAPS sounding retrieval location at Haywards Heath, West Sussex, UK.

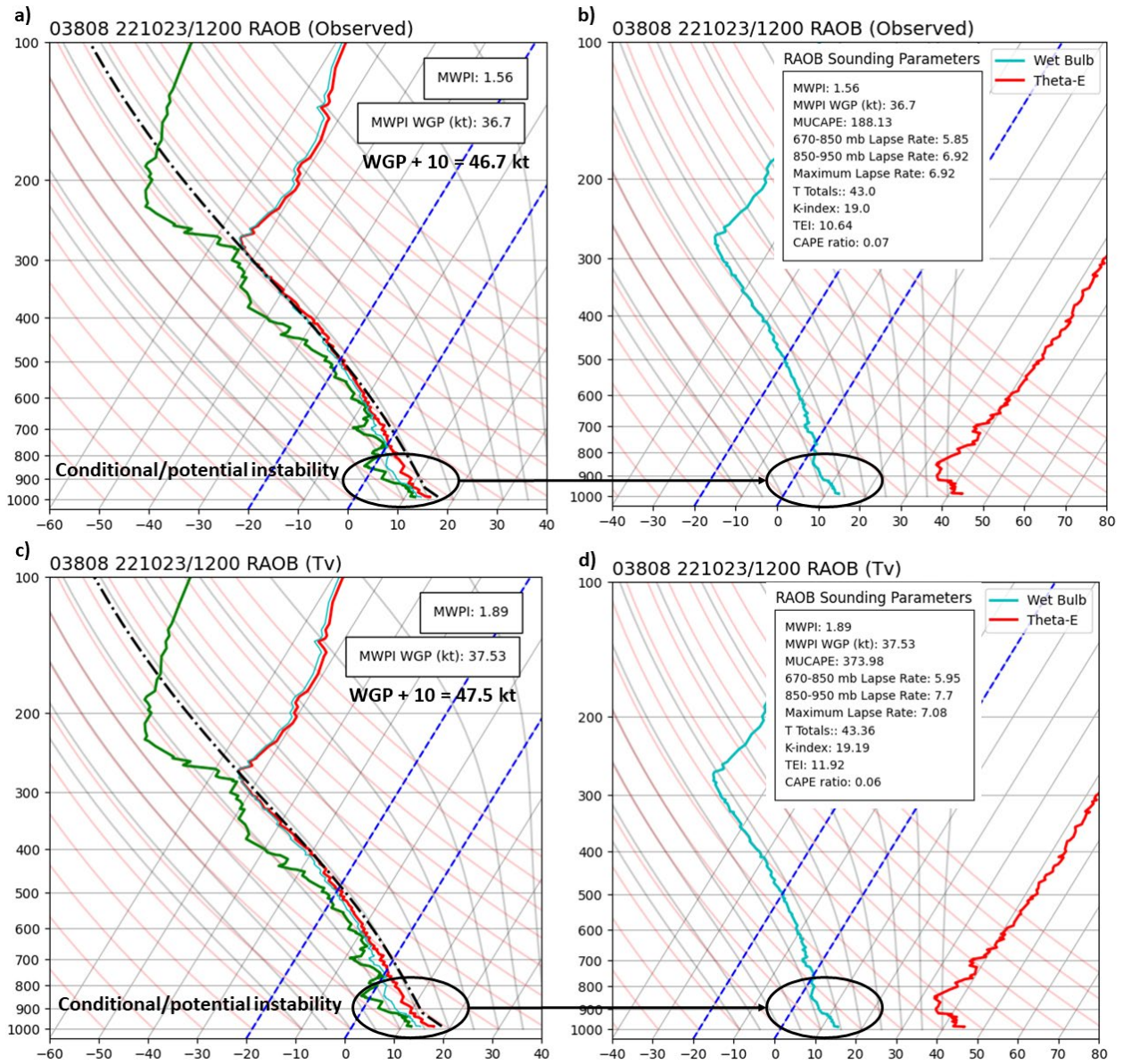


Figure 6. a) RAOB sounding profile at Camborne, Cornwall, UK at 1200 UTC 23 October 2023 with b) associated profiles of wet bulb temperature and equivalent potential temperature (theta-e) derived from the RAOB temperature and dewpoint profiles. c) RAOB sounding profile at Camborne with the virtual temperature calculation applied and b) associated profiles of wet bulb temperature and equivalent potential temperature (theta-e) derived from the RAOB virtual temperature and dewpoint profiles. Red curves and green curves represent the temperature and dewpoint soundings in degrees Celsius ( $^{\circ}\text{C}$ ), respectively. “MUCAPE” is most unstable parcel CAPE in  $\text{J kg}^{-1}$ , “MWPI” represents the Microburst Windspeed Potential Index, and “WGP” represents wind gust potential derived from the MWPI in knots (kt). The additive factor of 10 knots represents one-third (1/3) of the forward storm motion yielding a total wind gust potential of 47.5 kt ( $24.4 \text{ ms}^{-1}$ ).

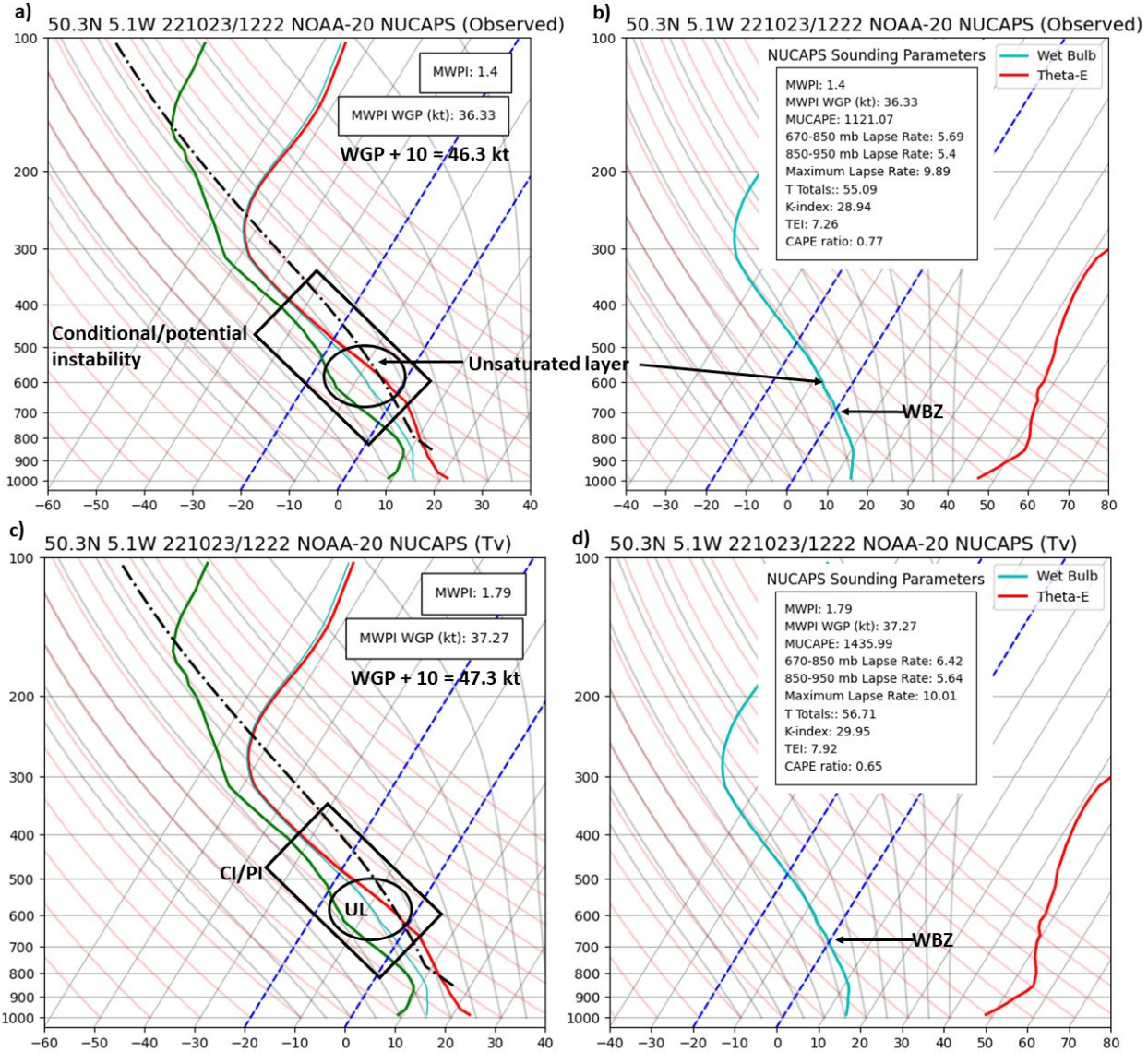


Figure 7. As in Fig. 6, but for the NOAA-20 NUCAPS sounding profile over Truro, Cornwall, UK at 1222 UTC 23 October 2022. “CI” denotes conditional instability, “PI” denotes potential instability, and “WBZ” represents the height of the wet bulb zero temperature. The additive factor of 10 knots represents one-third (1/3) of the forward storm motion yielding a total wind gust potential of 47.3 kt ( $24.3 \text{ ms}^{-1}$ ).

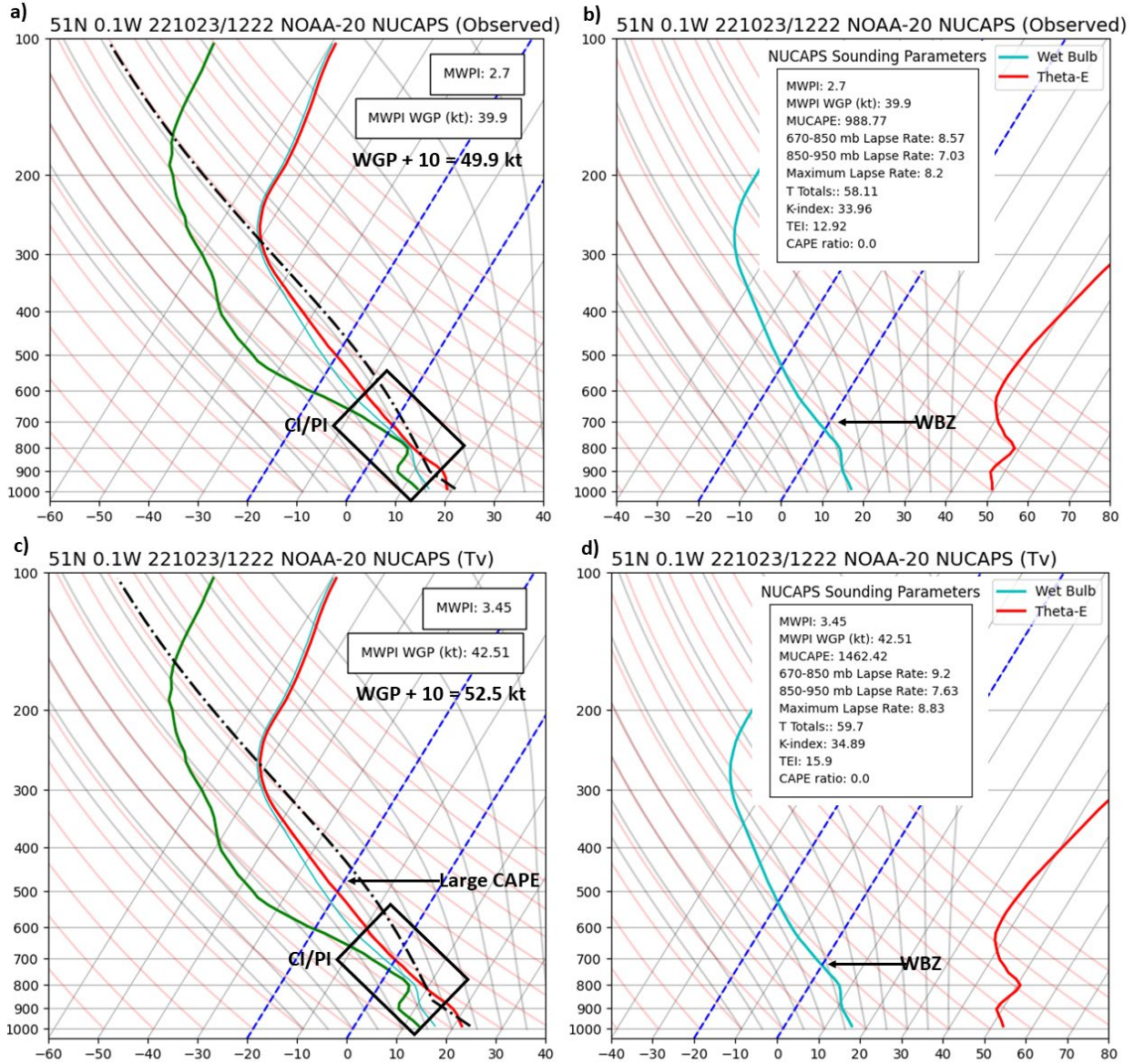


Figure 8. As in Fig. 6, but for the NOAA-20 NUCAPS sounding profile over Haywards Heath, West Sussex, UK at 1222 UTC 23 October 2022. “CI” denotes conditional instability, “PI” denotes potential instability, and “WBZ” represents the height of the wet bulb zero temperature. The additive factor of 10 knots represents one-third (1/3) of the forward storm motion yielding a total wind gust potential of 52.5 kt ( $27 \text{ ms}^{-1}$ ).

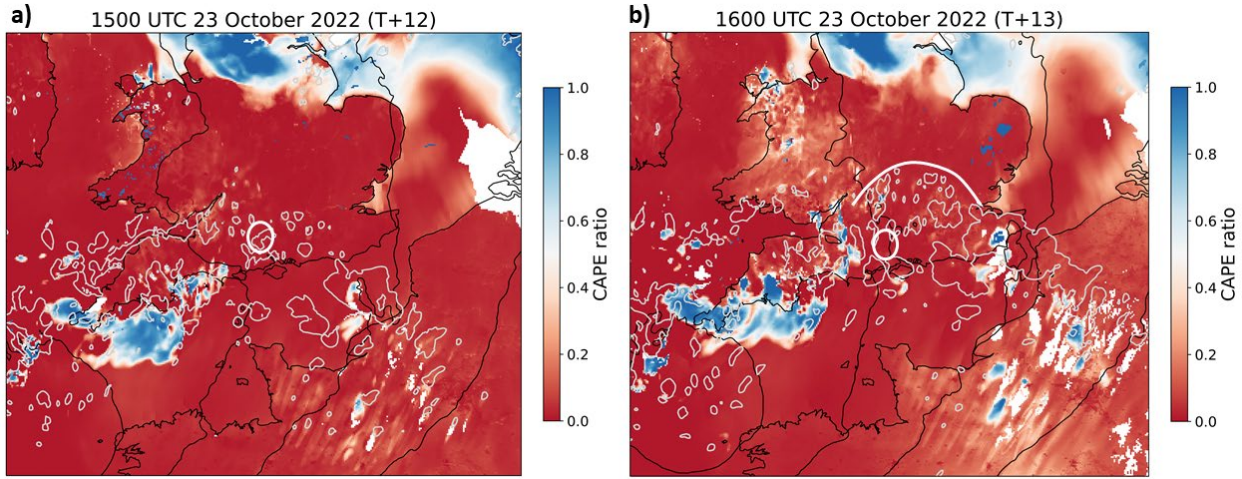


Figure 9. CAPE ratio diagnostic ( $1 - (\text{SBCAPE}/\text{MUCAPE})$ ) map from the UM forecasts of the 23 October 2022 QLCS: a) 1500 UTC and b) 1600 UTC. Reds indicate environments suitable for surface-based convection, blues indicate environments suitable for elevated convection. The gray contours show the 30 dBZ model reflectivity, and the black contours the MSLP. The white circle marks the location of downburst occurrence at Middle Wallop while the white arc represents the leading edge of the bowing segment of the MCS over the Midlands.

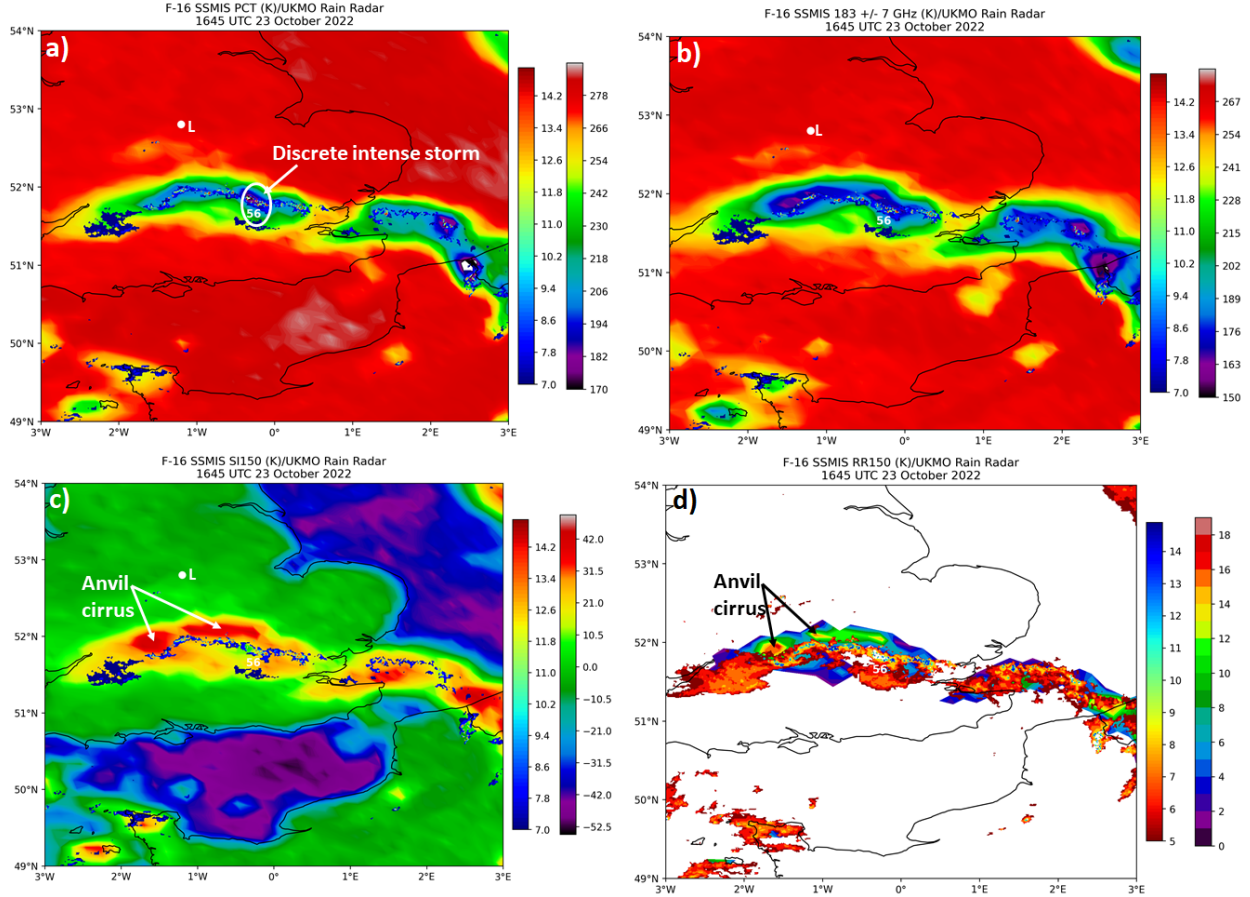


Figure 10. F-16 SSMIS a) polarization-corrected temperature (PCT, K), b) 183  $\pm$  7 GHz brightness temperature (K), c) 150 GHz scattering index (SI), and d) 150 GHz-channel derived rainfall rate (RR150) with overlying UKMO radar rainfall rate at 1645 UTC 23 October 2023. “L” marks the NUCAPS sounding retrieval location at Loughborough, Leicestershire, UK. “56” represents the 56-kt ( $28.8 \text{ ms}^{-1}$ ) downburst wind gust recorded at the Phoenix Model Club WeatherFile station in London Colney, Hertfordshire, UK.

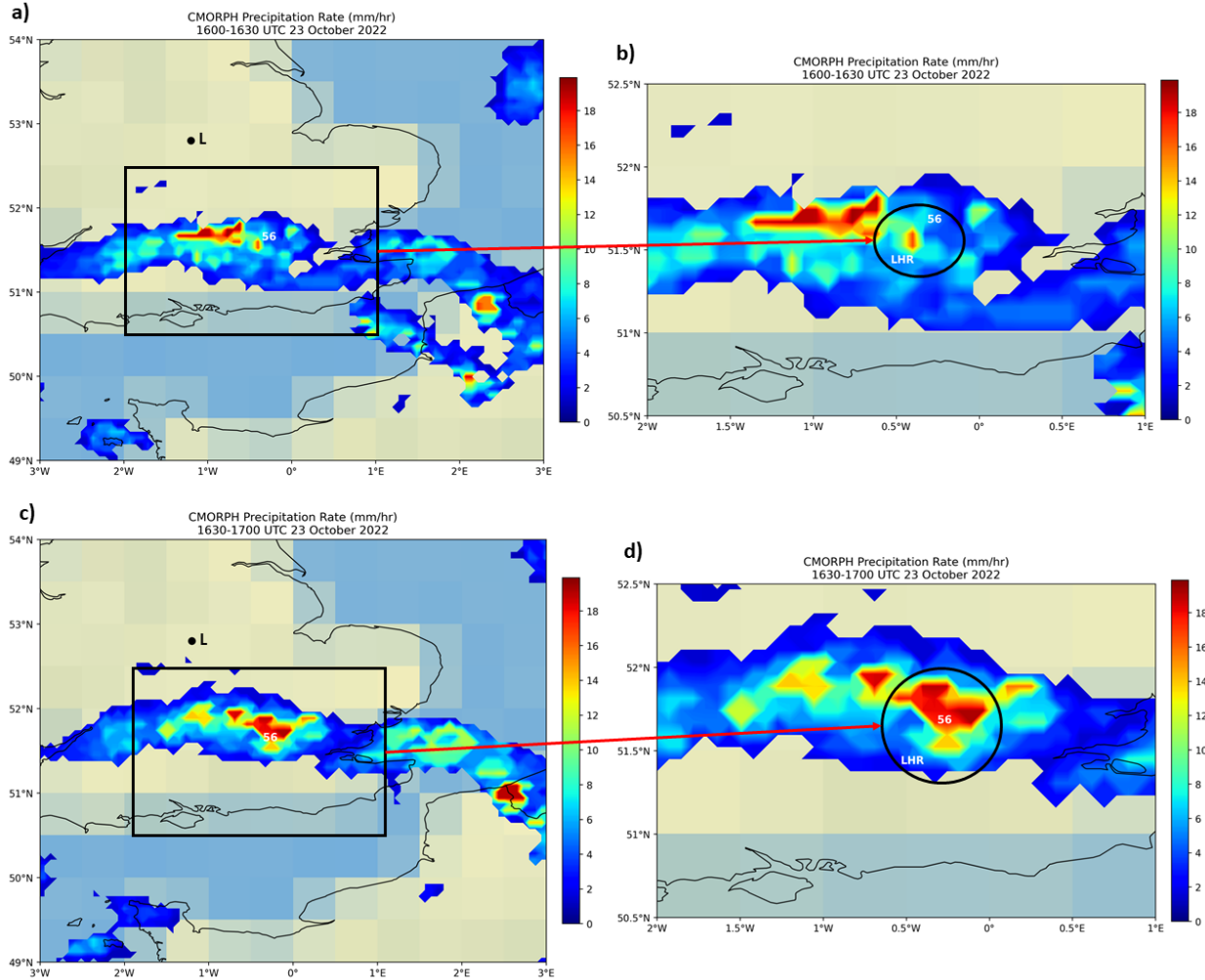
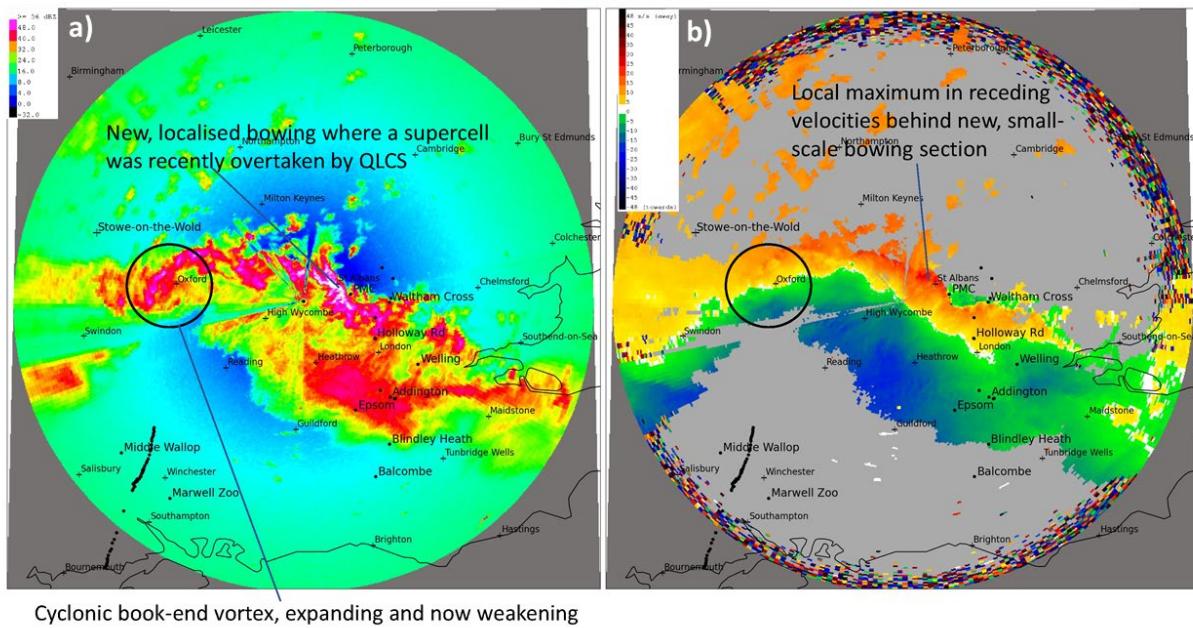


Figure 11. CMORPH precipitation rate (mm/hr) on 23 October 2022 at a) 1600-1630 UTC and c) 1630–1700 UTC; and CMORPH precipitation rate gradient at b) 1600-1630 UTC and d) 1630-1700 UTC. “L” marks the NUCAPS sounding retrieval location at Loughborough, Leicestershire, UK. “56” represents the 56-kt ( $28.8 \text{ ms}^{-1}$ ) downburst wind gust recorded at the Phoenix Model Club WeatherFile station in London Colney, Hertfordshire, UK, and “LHR” represents the location of London Heathrow Airport.

1631 UTC



1701 UTC

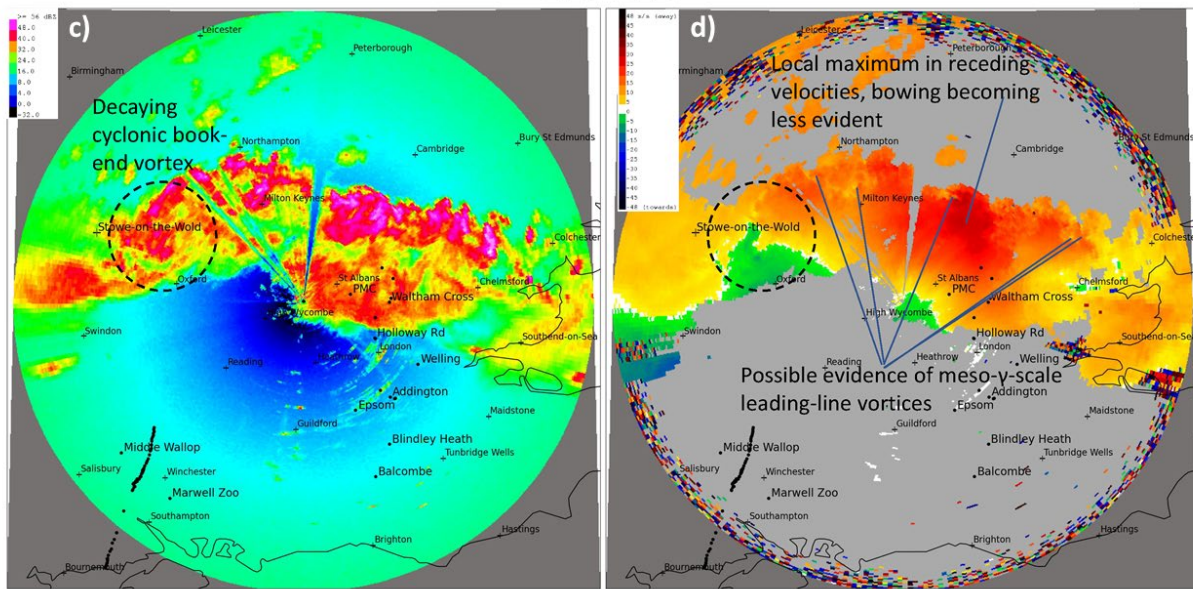


Figure 12. Chenies, UK Doppler radar a) reflectivity and b) velocity at 1631 UTC; c) reflectivity and d) velocity at 1701 UTC 23 October 2022. Black dots mark the location of reported damage. "PMC" represents the location of the 56-knot downburst wind gust recorded at the Phoenix Model Club WeatherFile station in London Colney, Hertfordshire, UK.

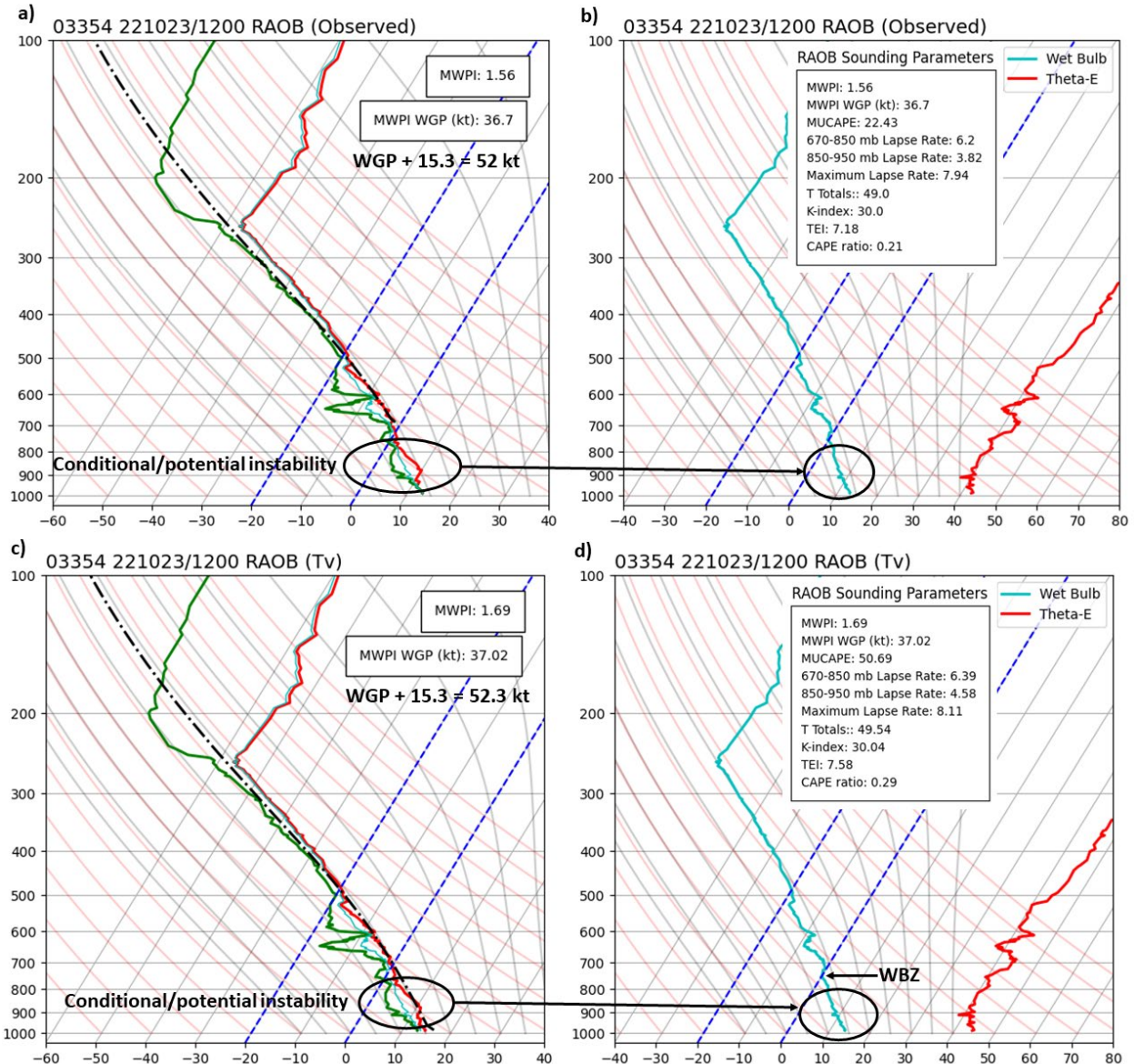


Figure 13. As in Fig. 6, but for the Nottingham RAOB sounding profile at 1200 UTC 23 October 2022. “WBZ” represents the height of the wet bulb zero temperature. The additive factor of 15.3 knots represents one-third (1/3) of the forward storm motion yielding a total wind gust potential of 52.3 kt ( $26.9 \text{ ms}^{-1}$ ).

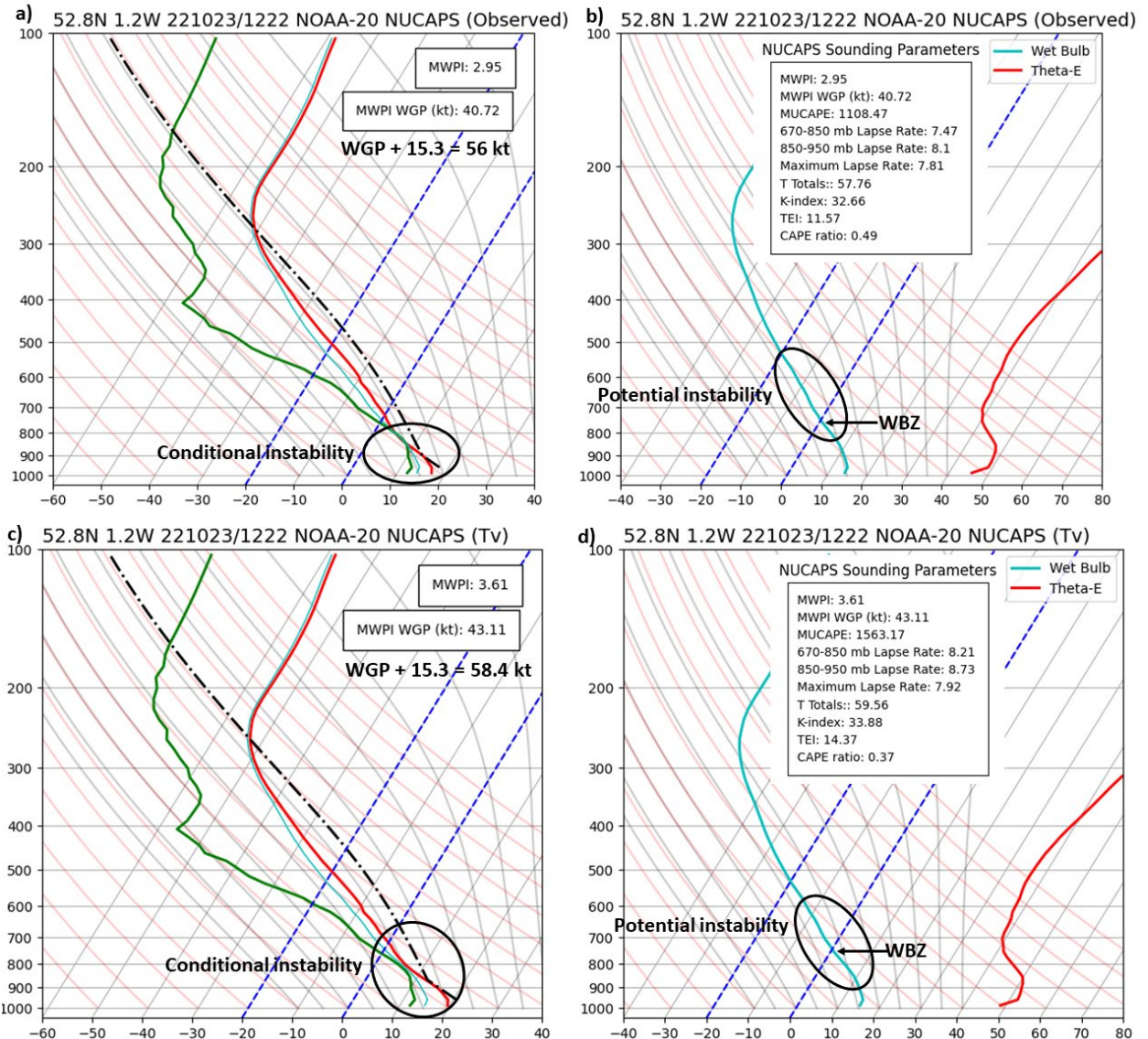


Figure 14. As in Fig. 6, but for the NOAA-20 NUCAPS sounding profile over Loughborough, Leicestershire, UK at 1222 UTC 23 October 2022. “WBZ” represents the height of the wet bulb zero temperature. The additive factor of 15.3 knots represents one-third (1/3) of the forward storm motion yielding a total wind gust potential of 58.4 kt ( $30 \text{ ms}^{-1}$ ).

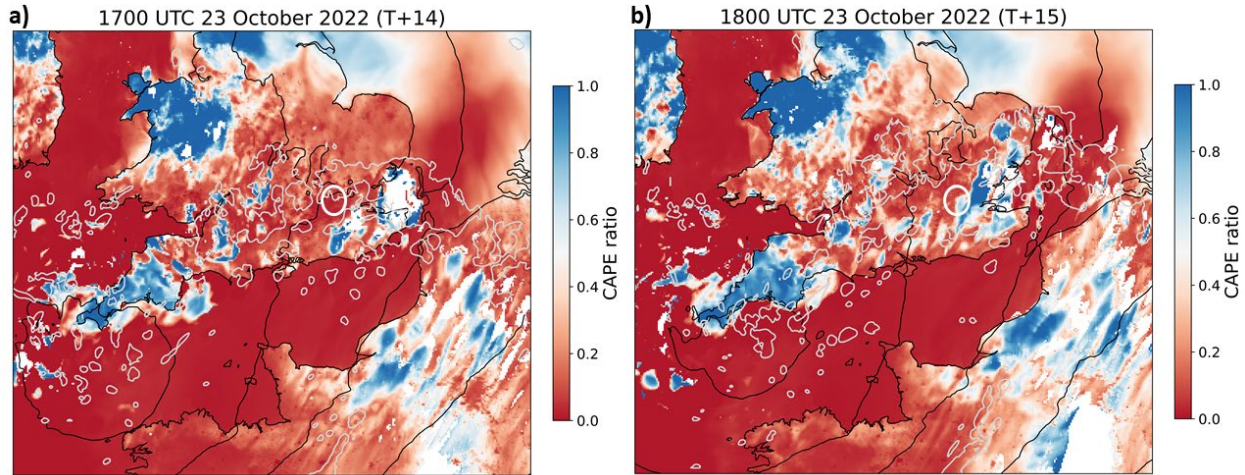


Figure 15. CAPE ratio diagnostic ( $1 - (\text{SBCAPE}/\text{MUCAPE})$ ) map from the UM forecasts of the 23 October 2022 QLCS: a) 1700 UTC and b) 1800 UTC. Reds indicate environments suitable for surface-based convection, blues indicate environments suitable for elevated convection. The gray contours show the 30 dBZ model reflectivity, and the black contours the MSLP. The white circle marks the location of downburst occurrence at London Colney, Hertfordshire.